ISSN: 2996-2544

Review Article

Journal of Research and Education

Hybrid PV-Geo-Aerothermal System for Self-Sufficient Energy Buildings

Carlos Armenta-Deu*

Faculty of Physics. Complutense University of Madrid, Spain

***Corresponding Author**
Carlos Armenta-Deu, Faculty of Physics. Complutense University of Madrid, Spain.

Submitted: 2025, Jul 25; **Accepted:** 2025, Aug 27; **Published:** 2025, Aug 29

Citation: Armenta-Deu, C. (2025). Hybrid PV-Geo-Aerothermal System for Self-Sufficient Energy Buildings. *J Res Edu, 3*(3), 01-22.

Abstract

This article analyzes the feasibility of a self-sufficient domestic energy installation powered by a hybrid renewable energy system consisting of a photovoltaic array and a domestic geothermal unit, supported by a battery bank to compensate for energy imbalances during periods of supply deficit. Energy consumption includes an aerothermal heat pump for heating, air conditioning, and domestic hot water, as well as appliances and accessories for the house's current operation. The analysis includes experimental validation of the self-sufficient system, considering the overall annual energy balance. The study analyzes the daily evolution of energy consumption and supply to determine the distribution of the energy balance over a shorter period and obtain a more precise analysis. The experimental results show that the designed system achieves a zero-energy balance with an accuracy of 0.02% for the overall annual energy balance. The monthly evaluation of the daily energy balance verifies that the selected battery bank compensates for the daily energy imbalance between supply and demand. The system design demonstrates the feasibility of the installation, provided the dwelling has sufficient space for the photovoltaic array and the geothermal unit. In the case studied, a 75 m² roof and a 50 m² plot of land provide enough space for a 26-panel photovoltaic array of 425 W each and a 3-kW geothermal unit for thermal energy supply.

Keywords: Building Energy Self-Sufficiency, Hybrid Renewable Energy System, Annual Net Zero Energy Balance

1. Introduction

Currently, many efforts focus on achieving energy self-sufficiency in buildings by using renewable energies as the primary source of energy supply [1-3]. The goals are to reduce energy consumption and dependence on fossil fuels, while minimizing the environmental impact of energy use for building air conditioning. The modern trend uses hybrid systems instead of single renewable sources since the hybridization supplies energy more continuously and improves the system efficiency [4-6]. Common hybridization systems in buildings include solar photovoltaic arrays, domestic wind turbines, heat pumps, electric thermal storage, and hydropower units [7-10]. The hybridization benefits from complementary energy sources, improving global efficiency and providing a reliable power supply [11-15].

Householders play a crucial role in advancing energy sufficiency since they represent a significant percentage of energy consumption in modern society. Nevertheless, their behavior depends not only on personal motivations but also on external factors such as policy mixes, specific technology availability, and economic profit [16-20]. Two opposing factors merge into the householder's decision to install a renewable energy hybrid system: the installation cost and the money saved in big cities, where power supply is produced at relatively low cost, the investment in a renewable energy system is a barrier to installing household self-sufficient energy systems [21-26]. On the other hand, the prospect of having energy at zero cost represents an attractive factor in favor of renewable energy in domestic installations [27-31].

Given the trade-off between a costly investment and an energy supply system with only maintenance costs, it is challenging to decide which system best suits a specific home. There is no single answer, as each house has unique characteristics and energy needs based on the residents' lifestyles [32-35]. Several proposals exist for achieving a sustainable and efficient household with zero external energy

dependence. These include single or hybrid systems, PV arrays with battery blocks solar, thermal systems with storage, domestic micro wind turbines solar thermal, and photovoltaic panels, PV systems connected heat pumps, domestic biomass devices and micro geothermal systems with PV arrays heat pump units or small wind turbines [36-56].

The above list shows the current state of the art; nevertheless, alternative solutions arise for supplying heat and electricity to detached and semi-detached houses. In this paper, we propose a hybrid system that combines a photovoltaic array for electric power supply with an aerothermal unit for sanitary water, heating, and air conditioning, and a geothermal system acting as a heat reservoir and complementary power source, heat, and electricity, when the PV array does not cover the house's energy requirements. The proposed power source combination benefits from a versatile power supply, the photovoltaic-aerothermal hybrid system, and an additional stable power source, the geothermal system, that stores energy for energy compensation when necessary.

2. Power Sources and Energy Requirements

The energy sources in a household come from heat and electricity for sanitary water, heating and air conditioning, and power supply for domestic appliances. In an energy self-sufficient system, the photovoltaic array supplies electricity for household lighting and electric appliances. Heating and air conditioning may operate on an electric current basis using a heat pump or a conventional gas boiler. The heating and air conditioning system may use wall radiators, underfloor heating, or fan-coil units [57-62]. Since the PV source does not operate during night and cloudy periods, the installation requires an electric storage system, currently a battery block. Thermal supply requires a storage unit because the aerothermal system operates under a photovoltaic array basis; therefore, when there is no solar radiation, the electric current from the PV power supply stops, and the aerothermal unit cannot continue working, interrupting the heat power supply for sanitary water, heating, and air conditioning. We can store thermal energy in several forms [63-64]; however, the typical form in a house is a hot water tank that preserves thermal energy for a short period. This situation generates a frequent heat power supply to compensate for thermal losses [65-66]. The thermal energy replacement proceeds from the aerothermal unit, which activates a heat exchange process to maintain the hot water tank temperature within limits.

An alternative solution for the hot water tank is to store thermal energy in the ground, as its temperature variations are low throughout the entire year, thereby minimizing the heat power required to maintain a constant temperature in the thermal reservoir. We, therefore, propose a ground thermal reservoir using a buried heat exchanger connected to the house's sanitary water circuit. In this way, the ground acts as a heat power supply when the aerothermal unit is not operational due to a PV power supply interruption. Another solution is a gravel-water pit which preserves thermal energy longer than a single water tank due to the gravel's higher heat capacity. In both cases, a ground reservoir or gravel-water pit, the sanitary water system requires an intermediate heat pump to raise the temperature from the thermal reservoir to the sanitary water circuit [67-72].

3. System Design and Characteristics

The proposed system consists of a set of 26 photovoltaic panels, lying on the tilted roof of a semi-detached house. Since the roof is oriented East and West, we divided the PV array into two groups of 13 panels for each orientation. Each panel has a peak power of 425 watts, resulting in an equivalent power of 8.288 kW for a south-oriented photovoltaic array with the same inclination as mentioned. Table 1 shows the technical characteristics of the PV panels.

Nominal Maximum Power (P_{max})	425 W
Operating Voltage (V_{mp})	38.25 V
Operating Current (I_{mp})	11.11 A
Open Circuit Voltage (V_{OC})	45.64 V
Short Circuit Current (I_{SC})	11.82 A
Module Efficiency	20.6%

Table 1: PV panel technical characteristics

The two strings of the PV array are connected to a 8.6 kW system with a double MPPT unit, one for every string. The input voltage is 500 VDC per string, and the maximum current is 11.11 A. The inverter is an island-type, operating off-grid for household energy self-sufficiency. The inverter includes a control module allowing the unit to connect to the house electric circuit, the battery block, the aerothermal unit, and the ground thermal heat pump. Table 2 shows the inverter technical characteristics.

DC Input data	
Maximum operating power	8600 W
Maximum power per MPPT/string	4300 W
Maximum voltage	1000 V
Activation voltage	170 V
Nominal operating voltage	500 V
AC Output data	
Maximum operating power	8600 W
Maximum current	37.4 A
Operating voltage	230 V
Operating voltage range	180-276 V
Performance data	
Power factor	1
Maximum efficiency	98%
Average efficiency	97.5%
MPPT efficiency	>99.9%
Power losses	< 1W

Table 2: Inverter technical characteristics

The battery block is a four 6.0 kW unit operating at 48 VDC nominal voltage, with a working range of 42-54 VDC [73]. The maximum delivered energy is 5.4 kW per unit, with a 10% reservoir for security reasons. The recommended and maximum discharge currents are 50 and 75 A. The battery charge is protected by a BMS, which controls voltage, current, and temperature of every battery cell. Table 3 shows the battery block characteristics.

Material	Lithium-Ferrophosphate
Nominal Voltage	48 V
Nominal Capacity	6.0 kW
Available Capacity	5.4 kW
Charge voltage	53.2 V
Working voltage range	42-54 V
Operating discharge current	62.5 A
Max. discharge current	93.75 A
Communication	RS232, RS482, CAN
Number of units	4
Working temp. range	0~55 ºC (charge)
	-20~55 ºC (discharge)
	-10~35 ºC (storage)
Lifespan	>6000 cycles

Table 3: Battery block technical characteristics

Figures 1 and 2 show the schematic representation of the system design.

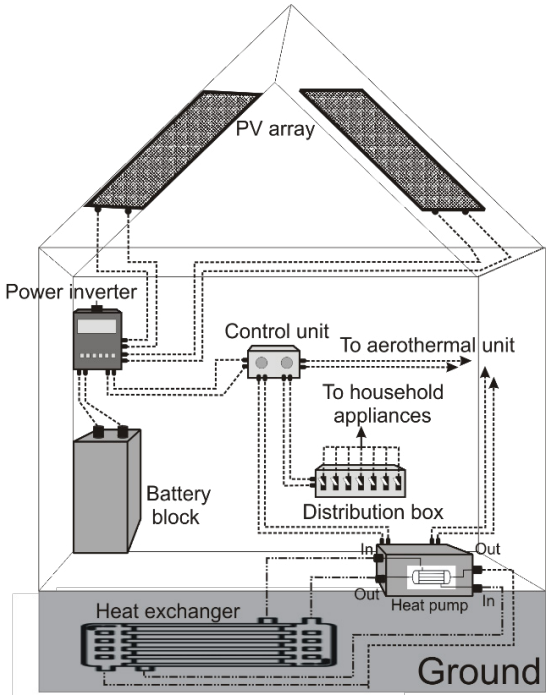

Figure 1: Layout of the electric distribution and the underground heat exchanger

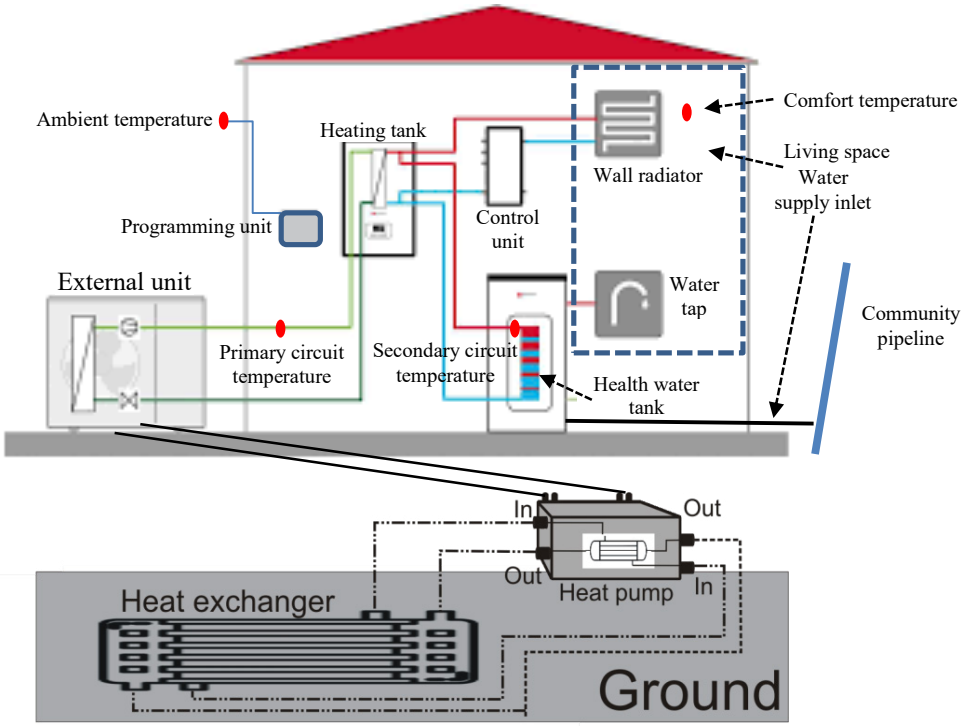

Figure 2: Layout of the thermal energy distribution (aerothermal unit and underground exchanger with assisting heat pump)

The aerothermal system is an air-water heat pump of 6 kW maximum power. The control unit that manages the aerothermal operation allows heating curve selection to increase or decrease the raising of water temperature. The heating curve selection responds to a PID control process [74]. The control unit also allows regulating hot water tank, and heating and air conditioning temperatures. We control the temperature regulation automatically through a home automation process assisted by Artificial Intelligence to optimize energy consumption [75]. Table 4 shows the aerothermal technical characteristics.

Electrical data	
Maximum operating power	6.0 kW
Power factor	1.0
Maximum operating current	23.3 A
Fan power consumption	160 W
Heat pump operating power	3-87 W
Thermal data	
Sanitary water temperature range	20-75 ºC
Water operating pressure range	0.05-0.30 MPa
Water flow range	995-2065 L/h
Heating flow range	45-150 L/h
Power supply in heating mode (primary circuit)	5.70 kW
Power supply in cooling mode (primary circuit)	7.80 kW
Power supply in heating mode (secondary circuit)	5.40-15.00 kW
Power supply in cooling mode (secondary circuit)	4.30-12.00 kW
Heating COP	4.20
Cooling COP	4.60
Effective power consumption (heating mode)	1.36 kW
Effective power consumption (cooling mode)	2.35 kW

Table 4: Aerothermal unit technical characteristics

The underground environment operates at variable temperatures depending on the season of the year; however, this variation is low, according to data from the geographical region where the house is located. Previous work shows that the ground temperature profile varies in the 19 °C to 25 °C range, with the minimum temperature corresponding to winter and the maximum to summer [76]; therefore, we can operate at an average temperature of 22 °C with a maximum temperature oscillation of ±3 °C. Since sanitary water operates in the 45ºC to 60ºC range, it is necessary to increase the underground reservoir temperature through a micro heat pump (Figure 1), whose principal goal is to maintain the health water tank at constant temperature, minimizing the dependence on the aerothermal unit, and improving the system's global efficiency. Because the temperature variation in the health water tank only occurs during sanitary water disposal, and this temperature variation is relatively low, the energy requirement to maintain constant the temperature of the health water tank is moderate; therefore, the micro heat pump power consumption is low, especially compared with the energy supply if the aerothermal unit is responsible to maintain the health water tank temperature constant. Table 5 shows the geothermal heat pump technical characteristics.

Available land area	71.5 m^2
Underground system area	50 m^2
Underground system depth	1.5 m
Heat pump power range	0.19-0.76 kW
Average heat pump operating	0.46 kW
Heating COP	3.5
Cooling COP	4.0
Maximum heating power supply	3.04 kW
Maximum cooling heating supply	1.86 kW

Table 5: Geothermal heat pump technical characteristics

3.Theoretical Background

In a standard household, we have two types of energy requirements: electric and thermal. Since electric power supply comes directly from the photovoltaic array, and the thermal energy proceeds from the aerothermal unit, and because the PV array and aerothermal unit efficiencies are different, we can express the household electric (P_{el}) and thermal (P_{th}) power requirement as in the following equations:

$$P_{el,c} = \frac{\xi_{el}\eta_{inv} + \xi_{el}^{L}}{t_{op}} \quad (1)$$

$$P_{th,c} = \frac{\xi_{th} + \xi_{th}^{L}}{t_{op} COP} \quad (2)$$

ξ_{el} and ξ_{th} correspond to the electric and thermal household energy requirements, η_{inv} is the inverter efficiency, ξ^{L}_{el} and ξ^{L}_{th} are the electric and thermal losses, *COP* is the aerothermal unit coefficient of performance, and t_{op} is the operation time. The subscript c accounts for consumption.

The electric energy requirements depend on the individual appliance power, its working time, and the number of elements, as in equation 3:

$$\xi_{el,c} = \sum_{i=1}^{n} \left(\sum_{j=1}^{m} P_j t_j \right)_i \quad (3)$$

P_j is the individual appliance power, and t_j is the working time. Subscript i accounts for the number of elements of any individual appliance of the same type, j.
On the other hand, thermal energy requirements include sanitary water and heating or air conditioning. To clarify, the thermal energy needs can be represented as shown in equation 4:

$$\xi_{th,c} = m_{SW} c_w \Delta T_{SW} + m_{air} c_{air} \Delta T_{air} \quad (4)$$

Electric and thermal losses derive from the classical expressions [77-78]:

$$\xi_{el}^{L} = \sum_{k} I_k R_k \; ; \; \xi_{th}^{L} = U_L S \Delta T_{room} \quad (5)$$

I and R are the current and electrical resistance of every wire in the electric installation, and k is the number of electric wires. U_L is the household global thermal losses coefficient, S is the household wall and roof surface, and ΔT_{room} is the temperature difference between the household interior and the environment.

Replacing Equations 3, 4, and 5 in Equations 1 and 2, we have:

$$P_{el,c} = \frac{1}{t_{op}} \left[\sum_{i=1}^{n} \left(\sum_{j=1}^{m} P_j t_j \right)_i \eta_{inv} + \sum_{k} I_k R_k \right] \quad (6)$$

$$P_{th,c} = \frac{1}{t_{op}} \left[\left(m_{SW} c_w \Delta T_{SW} + m_{air} c_{air} \Delta T_{air} \right) + U_L S \Delta T_{room} \right] \quad (7)$$

Converting power into energy:

$$\xi_{el,c} = \left[\sum_{i=1}^{n} \left(\sum_{j=1}^{m} P_j t_j \right)_i \eta_{inv} + \sum_{k} I_k R_k \right] \quad (8)$$

$$\xi_{th,c} = m_{SW} c_w \Delta T_{SW} + m_{air} c_{air} \Delta T_{air} + U_L S \Delta T_{room} \quad (9)$$

Electric power is supplied by the photovoltaic array and the battery block. The PV system supplies energy as a function of the solar radiation level, which is variable throughout the day; therefore:

$$P_{el,s}^{PV} = f_{or} N_{PV} \frac{G}{1000} (PV)_M \quad (10)$$

$(PV)_M$ is the photovoltaic panel peak power, G is the solar radiation, N_{PV} is the number of photovoltaic panels, and f_{or} is the correction factor due to the East-West orientation of the PV array. The superscript PV indicates that the power supply corresponds to for the photovoltaic array.

Converting power into energy, we have:

$$\xi_{el,s}^{PV} = f_{or} N_{PV} \frac{(PV)_M}{1000} \sum_l G_l \tag{11}$$

The subscript l corresponds to the operating time interval, and G_l is the solar radiation corresponding to this interval.

The time interval depends on the measuring protocol and accuracy of the data recording system; this time interval can be as low as a fraction of a second. However, in current practice, to avoid excessive data volume, the solar radiation is averaged over an hour; therefore, Equation 11 converts into:

$$\xi_{el,s}^{PV} = f_{or} N_{PV} \frac{(PV)_M}{1000} \sum_{t=1}^{24} G_t \tag{12}$$

The subscript t corresponds to the daily hour interval, and G_t is the average solar radiation over this hour. The subscript s indicates energy supply.

Thermal energy proceeds from the aerothermal unit and the underground reservoir. In the case of the aerothermal unit, we can express the thermal energy as:

$$\xi_{th,s}^{aero} = \xi_{th,c} = \xi_{el,s}^{aero} (COP)_{aero} \tag{13}$$

$\xi_{el,s}^{aero}$ is the fraction of electric energy generated by the PV array to produce thermal energy in the aerothermal unit heat pump. $(COP)_{aero}$ is the aerothermal unit coefficient of performance for heating or air conditioning.

If we convert thermal energy into electrical at the aerothermal unit, replacing Equation 9 in Equation 13, we obtain:

$$\xi_{el,s}^{aero} = \frac{m_{SW} c_w \Delta T_{SW} + m_{air} c_{air} \Delta T_{air} + U_L S \Delta T_{room}}{(COP)_{aero}} \tag{14}$$

Because we use the geothermal reservoir to replace thermal energy in the healthy water tank, Equation 14 should be expressed in the following way:

$$\xi_{el,s}^{aero} = \frac{m_{air} c_{air} \Delta T_{air} + U_L S \Delta T_{room}}{(COP)_{aero}} \tag{15}$$

The supplied energy by the geothermal heat pump is, therefore, given by:

$$\xi_{el,s}^{geo} = \frac{m_{SW} c_w \Delta T_{SW}}{(COP)_{geo}} \tag{16}$$

We can obtain the electric energy balance by comparing the power supply from the PV array and the battery block with the household, aerothermal and geothermal heat pump electric energy consumption.

The battery block health is critical since it represents the backup system that guarantees the household operational viability in case the PV array does not supply enough power to cover the household energy demand. If the electric energy balance is negative, the batteries block discharges, supplying energy to compensate for the energy deficit. If positive, the batteries block charges. Therefore, the battery output/input energy is given by:

a) Battery discharge process

$$\xi_{el,s}^{bat}\Big|_d = \left[\sum_{i=1}^{n} \left(\sum_{j=1}^{m} P_j t_j \right)_i \eta_{inv} + \sum_k I_k R_k \right] + \frac{m_{air} c_{air} \Delta T_{air}}{(COP)_{aero}} + \frac{+U_L S \Delta T_{room}}{(COP)_{geo}} - \xi_{el,s}^{PV} \tag{17}$$

b) Battery charge process

$$\xi_{el,s}^{bat}\Big|_{ch} = \xi_{el,s}^{PV} - \left[\sum_{i=1}^{n}\left(\sum_{j=1}^{m} P_j t_j\right)_i \eta_{inv} + \sum_k I_k R_k\right] - \frac{m_{air} c_{air} \Delta T_{air}}{(COP)_{aero}} - \frac{U_L S \Delta T_{room}}{(COP)_{geo}} \quad (18)$$

In terms of electric parameters:
a) Battery discharge process

$$\xi_{el,s}^{bat}\Big|_{h} = V_D I_D t_D \quad (19)$$

b) Battery charge process

$$\xi_{el,s}^{bat}\Big|_{h} = V_{ch} I_{ch} t_{ch} \quad (20)$$

V is the battery voltage, I is the current, and t is the operating time. Subscripts D and ch account for discharge and charge processes.

During the battery charge or discharge process, the remaining energy increases or decreases, modifying the state of charge of the battery (SOC) according to:

$$SOC = 1 - DOD = 1 - \sum_{y=1}^{z} \frac{(I_D t_D)_y}{C_{bat}} \quad (21)$$

For the discharge process, and:

$$SOC = \sum_{y=1}^{z} \frac{(I_{ch} t_{ch})_y}{C_{bat}} \quad (22)$$

For the charge process.
C_{bat} accounts for the battery block capacity, and subscript z for the number of charge/discharge processes.
Since the battery capacity changes with discharge current, Equations 21 and 22 convert into:

$$(SOC)_D = 1 - \sum_{y=1}^{z} \frac{(I_D t_D)_y}{C_n f_C} \quad (23)$$

$$(SOC)_{ch} = \sum_{y=1}^{z} \frac{(I_{ch} t_{ch})_y}{C_n f_C} \quad (24)$$

f_C represents the battery capacity correction factor, given by [79]:

$$f_C = 0.9541(t_D)^{0.0148} = 0.9541\left(\frac{I_D}{C_n}\right)^{0.0148} \quad (25)$$

C_n is the battery nominal capacity, corresponding to the delivered charge in the standard discharge time.

Replacing Equation 25 in Equations 23 and 24:

$$(SOC)_D = 1 - \frac{1}{0.9541} \sum_{y=1}^{z} \left[\left(\frac{I_D}{C_n}\right)^{1.9852}\right]_y \quad (26)$$

$$(SOC)_{ch} = \frac{1}{0.9541}\sum_{y=1}^{z}\left[\left(\frac{I_D}{C_n}\right)^{1.9852}\right]_y \quad (27)$$

Applying the Ohm's law:

$$(SOC)_D = 1 - \frac{1}{0.9541}\sum_{y=1}^{z}\left[\left(\frac{1}{C_n}\right)^{1.9852}\left(\frac{\xi_{bat}}{V_{bat}}C_n\right)^{1.9852/2}\right]_y = 1 - \frac{1}{0.9541}\sum_{y=1}^{z}\left[(C_n)^{-0.9926}\left(\frac{\xi_{bat}}{V_{bat}}\right)^{0.9926}\right]_y \quad (28)$$

$$(SOC)_{ch} = \frac{1}{0.9541}\sum_{y=1}^{z}\left[\left(\frac{I_D}{C_n}\right)^{1.9852}\right]_y = \frac{1}{0.9541}\sum_{y=1}^{z}\left[(C_n)^{-0.9926}\left(\frac{\xi_{bat}}{V_{bat}}\right)^{0.9926}\right]_y \quad (29)$$

Now, replacing Equations 17 and 18 in Equations 28 and 29:

$$(SOC)_D = 1 - \frac{1}{0.9541}\sum_{y=1}^{z}\left[(C_n)^{-0.9926}\left(\frac{\left[\sum_{i=1}^{n}\left(\sum_{j=1}^{m}P_j t_j\right)\eta_{inv} + \sum_k I_k R_k\right] + \frac{m_{air}c_{air}\Delta T_{air}}{(COP)_{aero}} + \frac{+U_L S\Delta T_{room}}{(COP)_{geo}} - \xi_{el,s}^{PV}}{V_{bat}}\right)^{0.9926}\right]_y \quad (30)$$

$$(SOC)_{ch} = \frac{1}{0.9541}\sum_{y=1}^{z}\left[(C_n)^{-0.9926}\left(\frac{\xi_{el,s}^{PV} - \left[\sum_{i=1}^{n}\left(\sum_{j=1}^{m}P_j t_j\right)\eta_{inv} + \sum_k I_k R_k\right] - \frac{m_{air}c_{air}\Delta T_{air}}{(COP)_{aero}} - \frac{U_L S\Delta T_{room}}{(COP)_{geo}}}{V_{bat}}\right)^{0.9926}\right]_y \quad (31)$$

We achieve the household energy sustainability if the battery state of charge remains positive, especially during the discharge process; therefore, the condition imposed is $(SOC)_D>0$, where the $(SOC)_D$ value derives from Equation 30.

The battery state of charge during charge is also important because it defines the starting point for the discharge process.

4. Experimental Tests and Results

We tested the household energy sustainability through experimental tests run for an entire year to compensate seasonal influence on the energy consumption. Table 6 shows the testing parameters of the experimental system.

Energy system	Photovoltaic
Subsystem	Parameter
PV array (strings 1 and 2)	Output voltage
	Output current
Inverter	Input DC power (string 1, 2, and total)
	Output AC voltage
	Output AC current
	Global output power
	Power factor
Energy system	Aerothermal
Subsystem	Parameter
Health water tank (HWT)	Input temperature (from network)
	Output temperature (to sanitary circuit)
Reservoir tank (RT)	Input temperature (from HWT)
	Output temperature (to HWT)
	Input temperature (from aerothermal unit)
	Output temperature (to aerothermal unit)
Aerothermal unit	Working pressure
	Water flow (primary circuit)
	Water flow (sanitary water circuit)
	Air temperature
	Electric energy consumption
	Thermal energy generation
	Coefficient of Performance (COP)
Energy system	Battery block
Subsystem	Parameter
Battery	Operational voltage
	Input-Output Current
	Input-Output charge
	Delivered power
	State of Charge
Energy system	Thermal storage System
Subsystem	Parameter
Heat pump	Working pressure
	Water flow (primary circuit)
	Water flow (sanitary water circuit)
	Air temperature
	Electric energy consumption
	Thermal energy generation
	Coefficient of Performance (COP)

Table 6: Experimental system testing parameters

Solar radiation measurements are collected by a SKS 1110 pyranometer sensor [80], which has a linearity error of less than 0.2%, current sensitivity of 50 μA/kW•m^{-2}, voltage sensitivity of 10 mV/kW•m^{-2}, and operational range of 0-5000 W/m^2. The response sensor time of 10 ns, assuring an immediate detection of any solar radiation variation.

The PV inverter is a chain monophasic unit, Greenheiss Series GH-IT [81], measuring the input voltage and current from the two PV array strings and the output voltage and current for the household electric circuit. The internal unit evaluates the power factor. The power factor has a 98.2% accuracy. The built-in energy counter operates in the range 0-9999 kWh, with a resolution of 0.01% and an accuracy

of 98.5%.

Battery and PV array electric parameters are measured using a high-resolution power analyzer, the PCE-PA-6000 [82], which has an accuracy of 0.1V and 10 mA for voltage and current detection, respectively. The power analyzer calculates the input and output power to and from the battery with an accuracy of 0.1 W for a measuring range below 1 kW, and of 1.0 W for a measuring range above 1 kW.

The aerothermal unit, Saunier Duval GeniaAir HA 15-6 O B3 [83], uses a high-resolution pressure gauge of 1Pa sensitivity to measure the working pressure, operating in the 0-2 MPa range. Temperature sensors are of the T-type, class 1, having a resolution of 0.5º C, and an operational range of -185 to 300º C. temperatures are continuously controlled through a multi-channel PicoLog data acquisition logger [84] connected to the control unit.

The geothermal heat pump, ecoForest model ecoGEO+AU6 [85], has similar characteristics to the aerothermal unit. Tests are run for one year, measuring values every minute and averaging the data hourly to match standard operating procedures. The control unit collects and records data, sending results to a connected computer for evaluation.

Showing hourly values for a whole year involves too much data. Instead, we display the average value of every day for each month.

The first group of tests results corresponds to the evolution of the photovoltaic energy supply (Figure 3). Every figure corresponds to a group of three months, corresponding to a yearly period centered on the solar solstice and equinox; February to April for the spring equinox, May to July for the summer solstice, August to October for the autumn equinox, and November to January for the winter solstice.

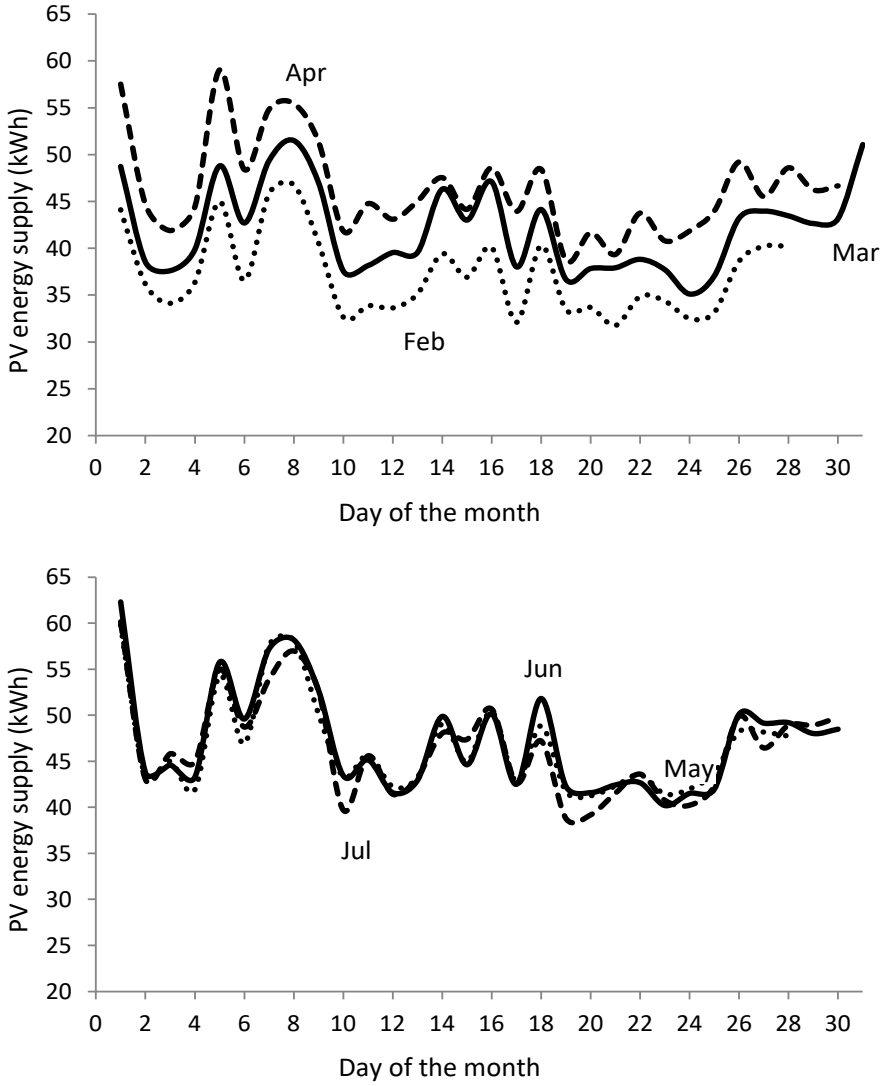

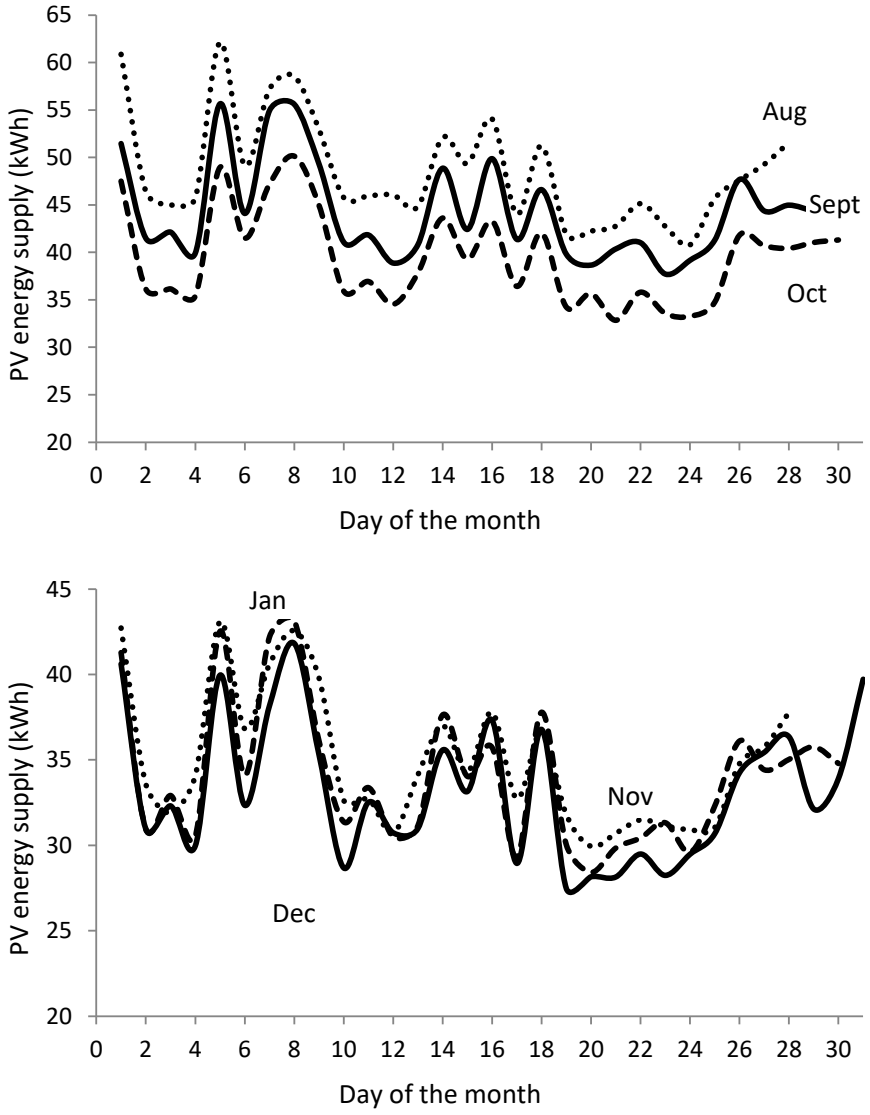

Figure 3: Daily evolution of the photovoltaic energy supply

Analyzing data from Figure 3, we observe that daily PV energy supply evolves from a minimum of 27.47 kWh to a maximum of 62.30 kWh. The PV evolution range varies depending on the season (Table 7).

Month period	Feb-Apr	May-Jul	Aug-Oct	Nov-Jan
Season	Spring	Summer	Autumn	Winter
PV power supply range (kW)	31.75-59.05	38.78-62.30	32.84-62.13	27.47-43.14
Average value (kW)	45.40	50.54	47.49	35.30
Deviation over yearly average (%)	8.49	20.78	13.48	15.64

Table 7: Seasonal average value and range for the PV energy supply

Figure 4 shows the monthly average value of the PV array energy supply. The dashed line corresponds to the yearly average value.

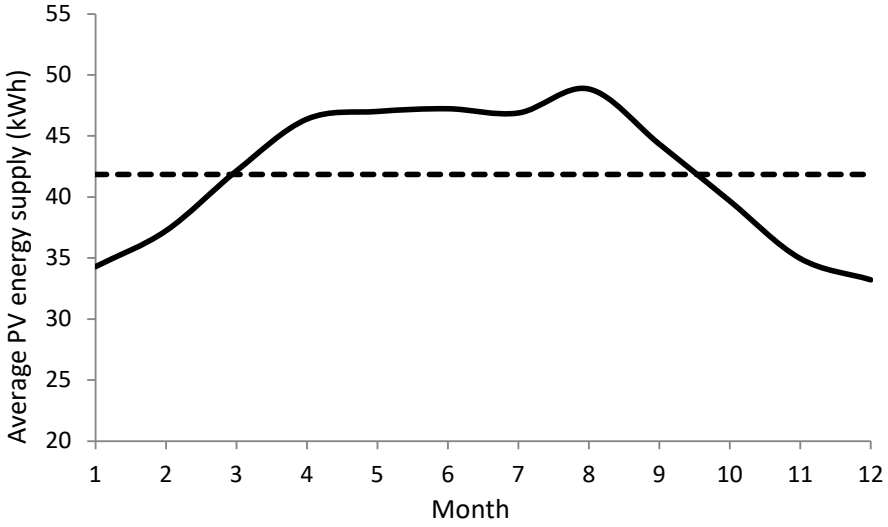

Figure 4: Monthly average value evolution of PV array energy supply

We notice that the monthly average PV energy supply evolution exceeds the yearly average value during the April through August period, and remains below the average from October to February. The second group of test results corresponds to the evolution of the household energy demand (Figure 5). Since sanitary water energy consumption depends on the geothermal heat pump supply, heating and air conditioning on the aerothermal unit, and electric consumption on the PV system, we divide the household energy demand into three groups, each corresponding to the above-mentioned energy consumptions.

Sanitary water is supplied by the health water tank, which requires thermal energy to regain the temperature level when hot water flows to the house. The power supply from the geothermal heat pump matches the energy demand corresponding to the hot water tank demand. We notice that daily thermal demand remained constant every day with a maximum deviation of 7.5%. On the other hand, the daily energy demand distribution also remained constant with a variation of less than 5%. Therefore, we can represent the geothermal heat pump power supply for a day, including daily deviation. Figure 5 shows the experimental results.

Analyzing the results from Figure 5, we notice that the geothermal heat pump supply depends on the season of the year, with a maximum in winter, and a minimum in summer, which agrees with expected values. The power supply operational range varies with the season of the year as shown in Table 8.

Season	Maximum power (kW)	Minimum power (kW)
Spring	0.464	0.232
Summer	0.398	0.199
Autumn	0.571	0.285
Winter	0.690	0.345

Table 8: Maximum and minimum geothermal heat pump power supply for the different seasons of the year

We notice that the values shown in Table 6 fall within the operational range for the geothermal heat pump indicated in Table 5.

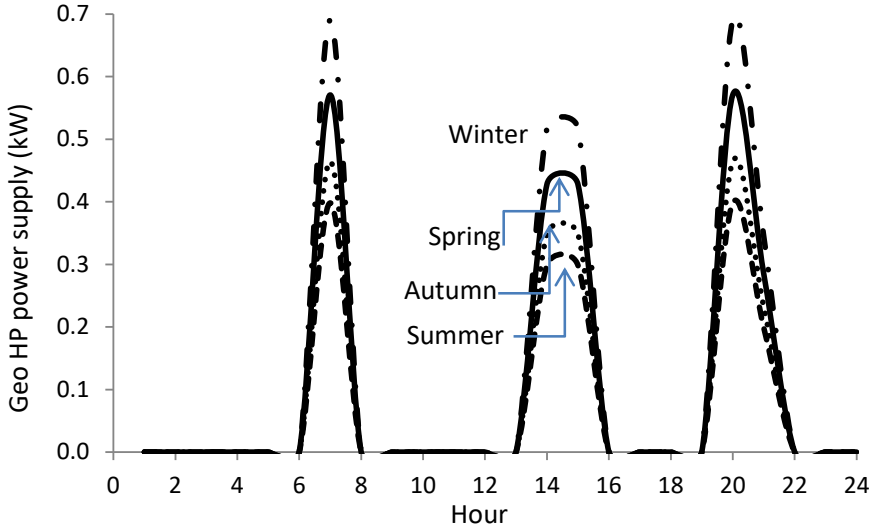

Figure 5: Geothermal Heat Pump daily power supply distribution

Integrating over the entire day, we obtain the geothermal heat pump daily energy consumption, obtaining a value of 2.76 kWh. Because the sanitary water use is regular, the heat pump energy consumption remains constant every day.

The third group of tests results corresponds to the evolution of the household thermal energy demand, heating and air conditioning (Figure 6). As in the case of the PV array energy supply, every figure corresponds to a group of three months, corresponding to a yearly period centered on the solar solstice and equinox; February to April for the spring equinox, May to July for the summer solstice, August to October for the autumn equinox, and November to January for the winter solstice.

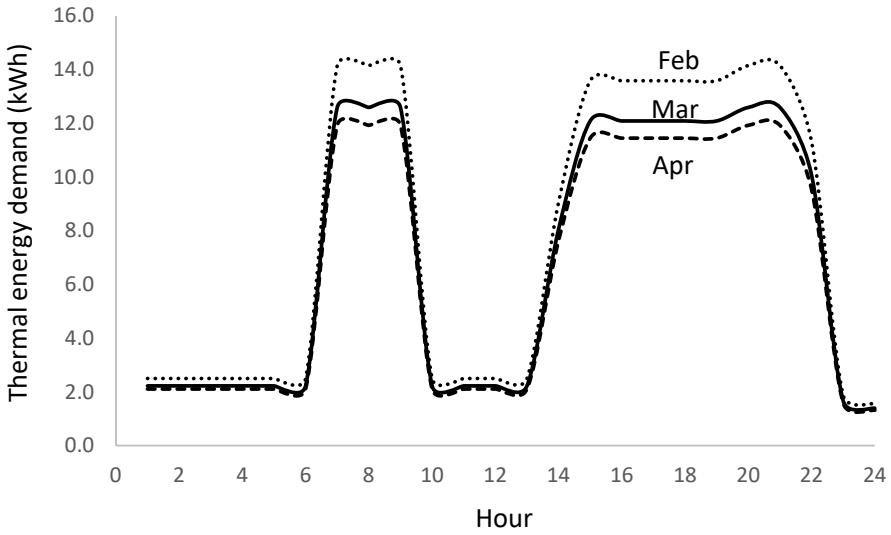

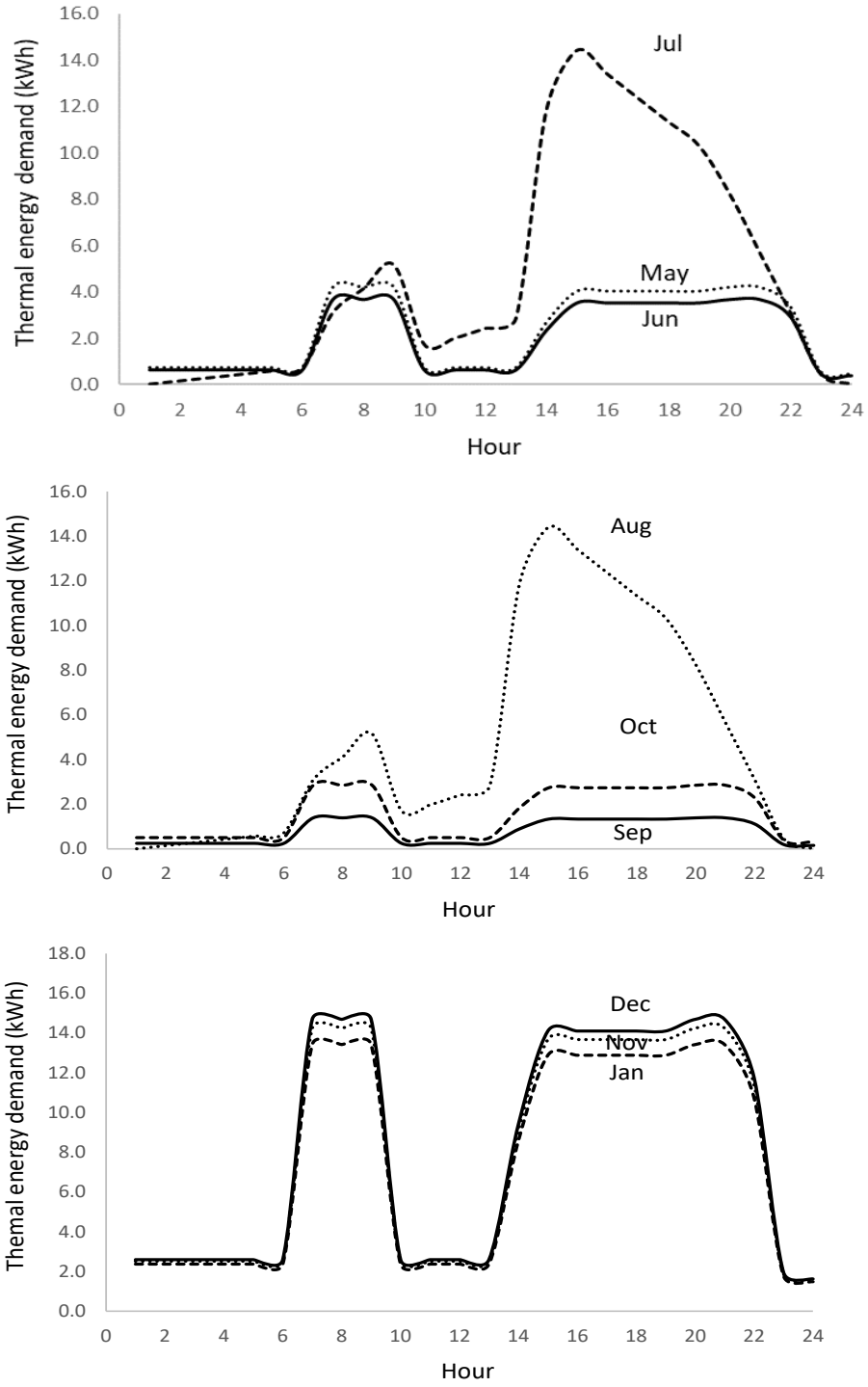

Figure 6: Hourly evolution of the household energy demand per month of the year

Heating operates from September to June, though in mild-temperature months, the heating energy demand is low. Nevertheless, we consider a heating contribution to the household energy demand during these months since the heating system is individual and not collective, meaning that the user may operate the heating system at will or automatically, generating the heating system activation if the inside temperature falls below the comfort level on any day during these months.

The analysis of household energy demand indicates that, from late autumn to early spring (November through April), the evolution is similar, with two peak daily periods: in the morning, 6 to 10 hours, and from early afternoon to near midnight, 14 to 22 hours. The rest of the day, energy demand is low due to the low or null human activity. On the other hand, in July and August, the energy demand

distribution is irregular, with a peak period near 3 p.m., and a slight slope from 3 p.m. to 10 p.m., due to air conditioning activation. The months of May, June, September, and October show a regular energy demand distribution, with slight differences between months. The energy demand in these months is much lower than in July and August because air conditioning consumes more energy than heating, and the operation time range is shorter.

Considering the monthly evolution of the energy consumption, we obtain (Figure 7):

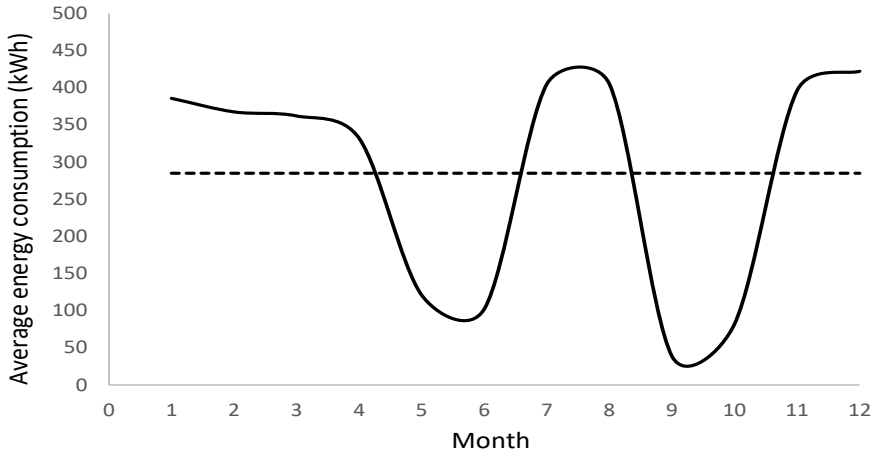

Figure 7: Monthly average value evolution of household energy demand (thermal)

We observe in Figure 7 that thermal energy demand evolves with the month of the year, following the climatic environment evolution, with maximum values in winter and summer, due to a higher demand in heating and air conditioning, and minimum values in May-June and September-October, corresponding to the mild climate in the operating zone.

Regarding the electrical energy consumption, we collected data from the control unit, obtaining the results shown in Figure 8. The data correspond to household appliances and accessories and do not include aerothermal or geothermal heat pumps, as their electric energy consumption corresponds with the previously analyzed thermal energy demand.

We only present daily hourly data, as the difference in daily electricity consumption throughout the year is negligible, less than 1%.

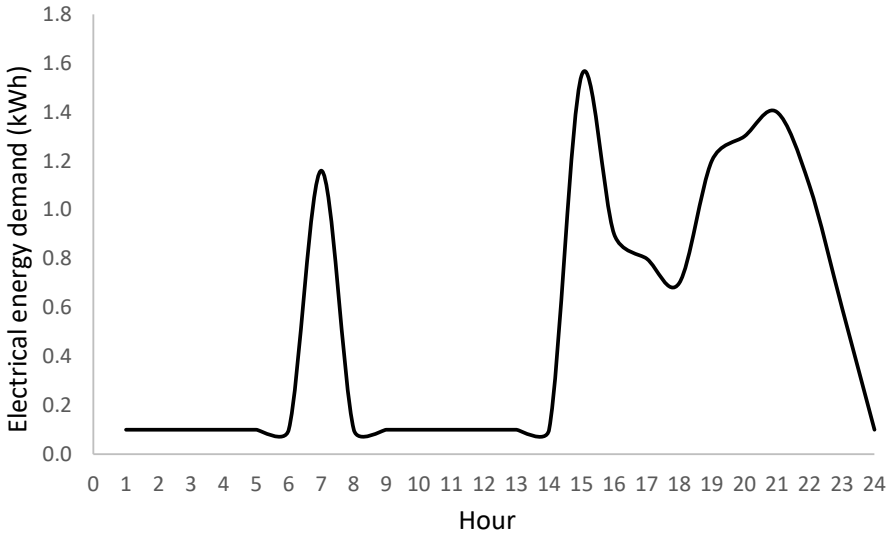

Figure 8: Daily hourly evolution of household energy demand (electrical)

The daily schedule corresponds to the specific habits of each family, with the highest levels of activity in the morning around 7:00 and from early afternoon, between 2:00 PM and midnight. This schedule may vary at any time if family habits change.

Once we have calculated all energy terms, we can determine the energy balance to establish the installation's sustainability. The battery bank is not included at this stage, as it only represents an energy storage system that supplies and receives energy from the installation to compensate for energy imbalances without affecting the overall energy balance. Equation 32 represents the overall energy balance.

Computing all energy terms, we obtain:

$$\xi_{ov} = \sum_i \left(\xi_{PV}\right)_i - \sum_j \left(\xi_{th}\right)_j - \sum_k \left(\xi_{geo}\right)_k - \sum_l \left(\xi_{el}\right)_l \tag{32}$$

$$\xi_{ov} = 24330.53 - 18921.59 - 1007.04 - 4395.93 = 5.97 kWh \tag{33}$$

The result of the energy balance shows a negligible deviation, less than 0.02%, respect to the zero-energy balance. This value guarantees the system sustainability and the household energy self-sufficiency.

However, the overall annual energy balance is not entirely accurate, as it masks potential hourly or daily energy imbalances; therefore, it is advisable to analyze the evolution of the hourly and daily energy balances. Since the battery bank operates daily, the battery hourly energy balance is not suitable, and the daily energy balance is the optimal option. Figure 9 shows the experimental results.

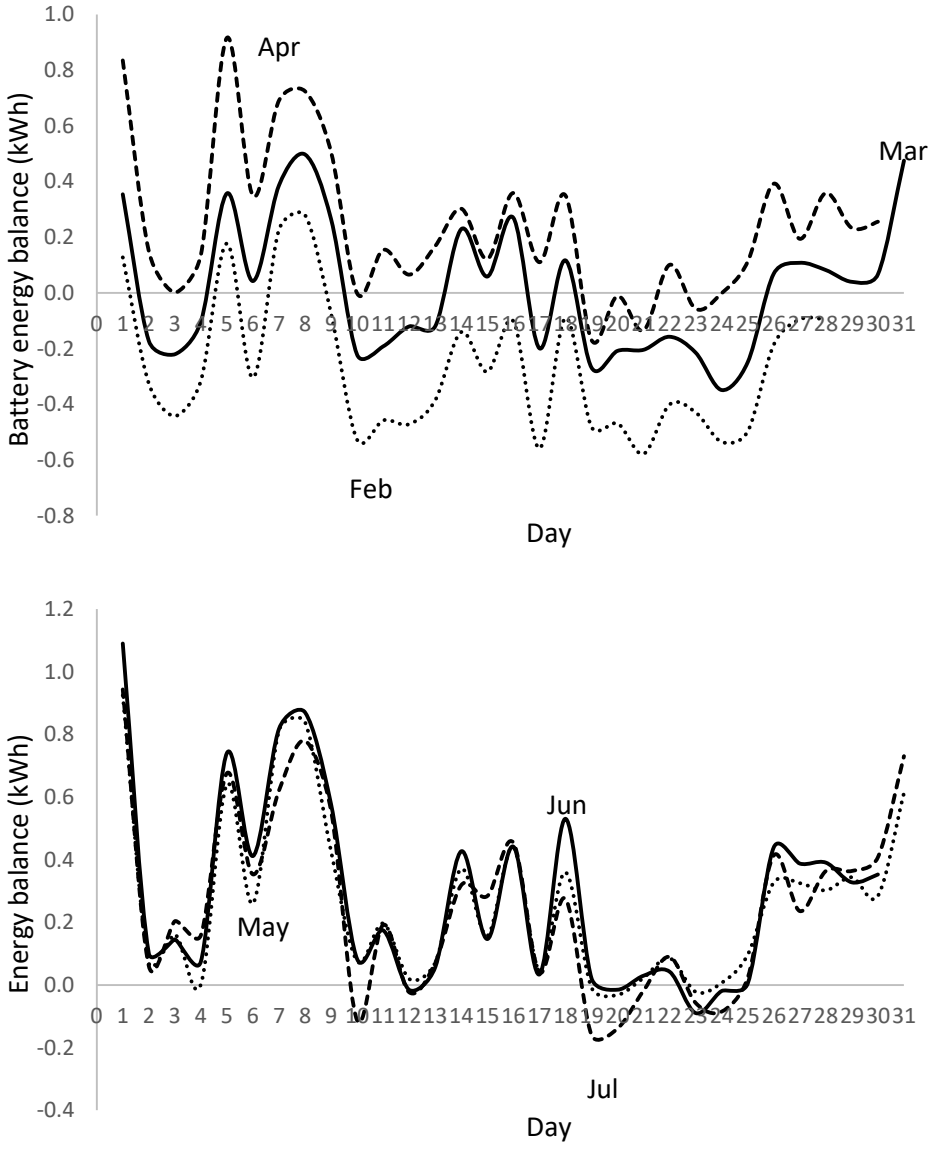

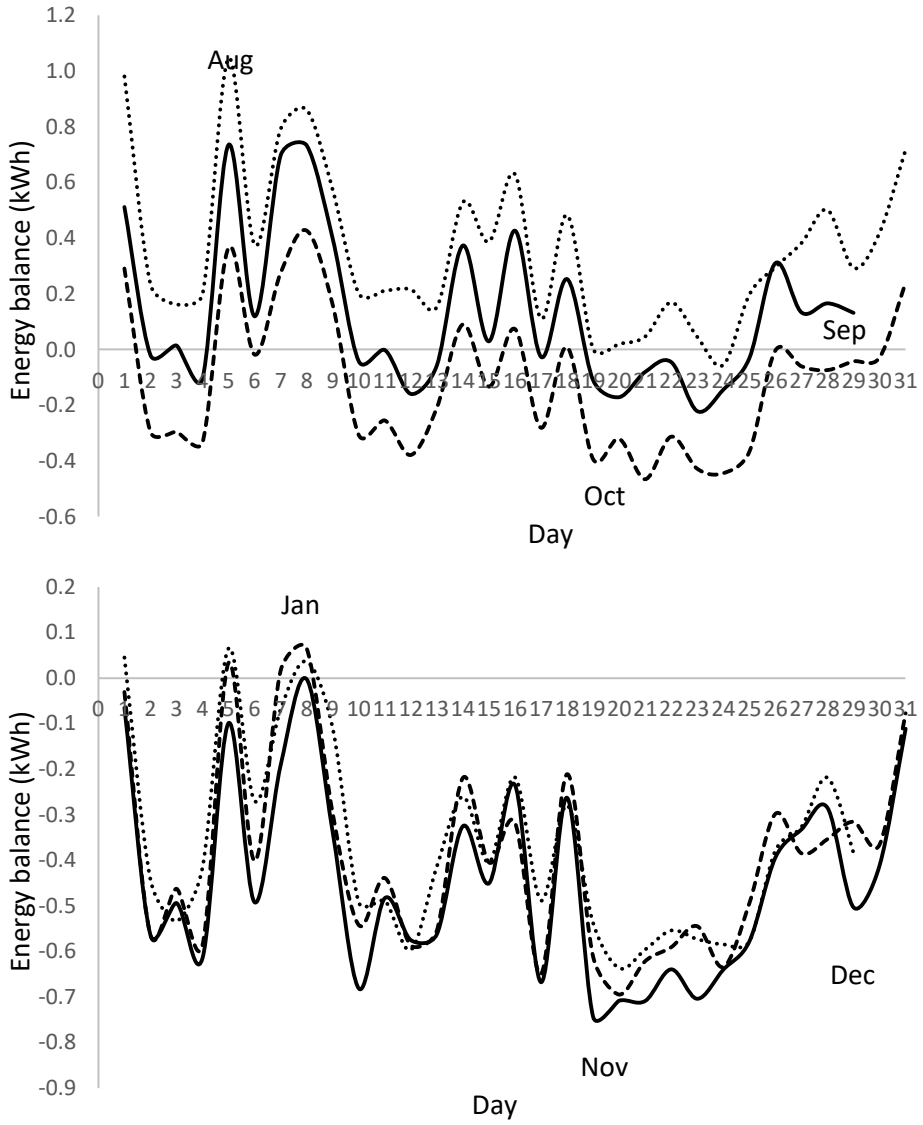

Figure 9: Battery daily energy balance

Applying values from Figure 9 to a battery block, the resulting capacity is (Table 9):

Month	Jan	Feb	Mar	Apr	May	Jun
Bat.cap. (kWh)	21.527	16.189	10.810	5.066	0.990	2.692
Month	Jul	Aug	Sep	Oct	Nov	Dec
Bat.cap. (kWh)	4.946	1.729	6.650	14.446	19.094	23.044

Table 9: Monthly battery capacity to compensate energy imbalances

Operating with a battery block of 6.0 kWh, the number of elements for the battery block is:

$$N_{bat} = \frac{\max(\xi_{bat})}{C_{bat}} = \frac{23.044}{6.0} = 3.84 \rightarrow 4 \quad (34)$$

Matching the selected number for the battery block in the storage system design (Table 3).

5. Conclusions

A single-family home, whether detached or semi-detached, can be energy self-sufficient through the renewable energy systems use. The application of a hybrid system—a photovoltaic array and a geothermal unit—in this study validates this claim.

The sustainability of energy installations requires the use of highly efficient systems to supply thermal energy, such as high-performance air-source and geothermal heat pumps. Using these systems reduces the electrical energy to produce thermal energy, minimizing the size of the photovoltaic system and allowing the photovoltaic installation to meet the house's energy needs.

A home that uses sustainable energy requires a battery bank with sufficient capacity to compensate for energy imbalances throughout the year, resulting from the variability in the photovoltaic system power supply and the variation in energy demand due to annual weather conditions variability.

Designing an energy-efficient system compatible with a home's self-consumption requires sufficient space for installing the photovoltaic system, the air source heat pump, and the geothermal heat pump with its heat exchanger. This configuration is feasible in single-family homes and semi-detached houses with a small adjacent plot of land and a terrace or rooftop with enough space for the photovoltaic system.

References

1. Orikpete, O. F., Ikemba, S., & Ewim, D. R. E. (2023). Integration of renewable energy technologies in smart building design for enhanced energy efficiency and self-sufficiency. *The Journal of Engineering and Exact Sciences, 9*(9), 16423-01e.
2. Del Pero, C. The Role of Photovoltaic Technology in Achieving Energy Self-Sufficiency in Residential Buildings. *Available at SSRN 4733998.*
3. Fedorczak-Cisak, M., Radziszewska-Zielina, E., Nowak-Ocłoń, M., Biskupski, J., Jastrzębski, P., Kotowicz, A., ... & Klemeš, J. J. (2023). A concept to maximise energy self-sufficiency of the housing stock in central Europe based on renewable resources and efficiency improvement. *Energy, 278,* 127812.
4. Gagliano, A., Tina, G. M., & Aneli, S. (2025). Improvement in Energy Self-Sufficiency in Residential Buildings Using Photovoltaic Thermal Plants, Heat Pumps, and Electrical and Thermal Storage. *Energies, 18*(5), 1159.
5. Di Leo, P., Spertino, F., Fichera, S., Malgaroli, G., & Ratclif, A. (2019, June). Improvement of self-sufficiency for an innovative nearly zero energy building by photovoltaic generators. In *2019 IEEE Milan PowerTech* (pp. 1-6). IEEE.
6. Laimon, M., & Yusaf, T. (2024). Towards energy freedom: Exploring sustainable solutions for energy independence and self-sufficiency using integrated renewable energy-driven hydrogen system. *Renewable Energy, 222*, 119948.
7. Chegari, B., Tabaa, M., Simeu, E., & El Ganaoui, M. (2024). Optimal energy management of a hybrid system composed of PV, Wind turbine, pumped hydropower storage and battery storage to achieve a complete energy self-sufficiency in residential buildings. *IEEE Access.*
8. Aneli, S., Arena, R., Tina, G. M., & Gagliano, A. (2023). Improvement of energy self-sufficiency in residential buildings by using solar-assisted heat pumps and thermal and electrical storage. *Sustainable Energy Technologies and Assessments, 60*, 103446.
9. Camargo, L. R., Gruber, K., Nitsch, F., & Dorner, W. (2019). Hybrid renewable energy systems to supply electricity self-sufficient residential buildings in Central Europe. *Energy Procedia, 158,* 321-326.
10. Ramirez Camargo, L., Nitsch, F., Gruber, K., Valdes, J., Wuth, J., & Dorner, W. (2019). Potential analysis of hybrid renewable energy systems for self-sufficient residential use in Germany and the Czech Republic. *Energies, 12*(21), 4185.
11. Nazari-Heris, M., & Asadi, S. (2023). Reliable energy management of residential buildings with hybrid energy systems. *Journal of Building Engineering, 71*, 106531.
12. Al-Rawashdeh, H., Al-Khashman, O. A., Al Bdour, J. T., Gomaa, M. R., Rezk, H., Marashli, A., ... & Louzazni, M. (2023). Performance analysis of a hybrid renewable-energy system for green buildings to improve efficiency and reduce GHG emissions with multiple scenarios. *Sustainability, 15*(9), 7529.
13. Juan, Y. K., Gao, P., & Wang, J. (2010). A hybrid decision support system for sustainable office building renovation and energy performance improvement. *Energy and buildings, 42*(3), 290-297.
14. Manwell, J. F. (2004). Hybrid energy systems. *Encyclopedia of energy, 3*(2004), 215-229.
15. Zohuri, B., Zohuri, & Quinn. (2018). *Hybrid energy systems* (pp. 1-38). Springer.
16. van der Kam, M., Lagomarsino, M., Parra, D., & Hahnel, U. J. (2025). Towards self-sufficiency: a socio-technical model to identify the transition pathways to flexible prosumers and the role of policy mixes. *Sustainability Science,* 1-19.
17. Strielkowski, W., Volkova, E., Pushkareva, L., & Streimikiene, D. (2019). Innovative Policies for Energy Efficiency and the Use of Renewables in Households. *Energies, 12*(7), 1392.
18. Kotilainen, K., & Saari, U. A. (2018). Policy Influence on Consumers' Evolution into Prosumers—Empirical Findings from an Exploratory Survey in Europe. *Sustainability, 10*(1), 186.
19. Stadler, M., Kranzl, L., Huber, C., Haas, R., & Tsioliaridou, E. (2007). Policy strategies and paths to promote sustainable energy systems—The dynamic Invert simulation tool. *Energy policy, 35*(1), 597-608.
20. Juan, Y. K., Gao, P., & Wang, J. (2010). A hybrid decision support system for sustainable office building renovation and energy performance improvement. *Energy and buildings, 42*(3), 290-297.
21. Nazari-Heris, M., Tamaskani Esfehankalateh, A., & Ifaei, P. (2023). Hybrid energy systems for buildings: a techno-economic-enviro

systematic review. *Energies, 16*(12), 4725.
22. Baseer, M. A., Alqahtani, A., & Rehman, S. (2019). Techno-economic design and evaluation of hybrid energy systems for residential communities: Case study of Jubail industrial city. *Journal of Cleaner Production, 237*, 117806.
23. Jaccard, M., & Dennis, M. (2006). Estimating home energy decision parameters for a hybrid energy—economy policy model. *Environmental Modeling & Assessment, 11*(2), 91-100.
24. Palm, J. (2018). Household installation of solar panels–Motives and barriers in a 10-year perspective. *Energy Policy, 113*, 1-8.
25. Kastner, I., & Matthies, E. (2016). Investments in renewable energies by German households: A matter of economics, social influences and ecological concern?. *Energy Research & Social Science, 17*, 1-9.
26. Eleftheriadis, I. M., & Anagnostopoulou, E. G. (2015). Identifying barriers in the diffusion of renewable energy sources. *Energy Policy, 80,* 153-164.
27. Rafique, M. M., Rehman, S., & Alhems, L. M. (2018). Developing zero energy and sustainable villages–A case study for communities of the future. *Renewable Energy, 127,* 565-574.
28. Alrashed, F., & Asif, M. (2012). Prospects of renewable energy to promote zero-energy residential buildings in the KSA. *Energy Procedia, 18,* 1096-1105.
29. Hongvityakorn, B., Jaruwasupant, N., Khongphinitbunjong, K., & Aggarangsi, P. (2024). Achieving Nearly Zero-Energy Buildings through Renewable Energy Production-Storage Optimization. *Energies, 17*(19), 4845.
30. Visa, I., Moldovan, M. D., Comsit, M., & Duta, A. (2014). Improving the renewable energy mix in a building toward the nearly zero energy status. *Energy and Buildings, 68,* 72-78.
31. Aruta, G., Ascione, F., Bianco, N., Iovane, T., Mastellone, M., & Mauro, G. M. (2023). Optimizing the energy transition of social housing to renewable nearly zero-energy community: The goal of sustainability. *Energy and Buildings, 282,* 112798.
32. Wróblewski, P., & Niekurzak, M. (2022). Assessment of the possibility of using various types of renewable energy sources installations in single-family buildings as part of saving final energy consumption in Polish conditions. *Energies, 15*(4), 1329.
33. Babatunde, O. M., Munda, J. L., & Hamam, Y. (2019). Selection of a hybrid renewable energy systems for a low-income household. *Sustainability, 11*(16), 4282.
34. Siksnelyte-Butkiene, I., Zavadskas, E. K., & Streimikiene, D. (2020). Multi-criteria decision-making (MCDM) for the assessment of renewable energy technologies in a household: A review. *Energies, 13*(5), 1164.
35. Cao, S., Hasan, A., & Sirén, K. (2013). Analysis and solution for renewable energy load matching for a single-family house. *Energy and buildings, 65,* 398-411.
36. Aşchilean, I., Cobîrzan, N., Bolboaca, A., Boieru, R., & Felseghi, R. A. (2021). Pairing solar power to sustainable energy storage solutions within a residential building: A case study. *International Journal of Energy Research, 45*(10), 15495-15511.
37. Nassereddine, M., Rizk, J., Nagrial, M., & Hellany, A. (2018, April). Battery sustainable PV solar house: Storage consideration for off grid. In *2018 Third International Conference on Electrical and Biomedical Engineering, Clean Energy and Green Computing (EBECEGC)* (pp. 34-38). IEEE.
38. Middelhauve, L., Baldi, F., Stadler, P., & Maréchal, F. (2021). Grid-aware layout of photovoltaic panels in sustainable building energy systems. *Frontiers in Energy Research, 8*, 573290.
39. Weiss, W. (2003). *Solar heating systems for houses: a design handbook for solar combisystems.* Earthscan.
40. Kumar, A. R., & Ramakrıshnan, M. (2022). A scoping review on recent advancements in domestic applications of solar thermal systems. *Journal of Thermal Engineering, 8*(3), 426-444.
41. Pirmohamadi, A., Dastjerdi, S. M., Ziapour, B. M., Ahmadi, P., & Rosen, M. A. (2021). Integrated solar thermal systems in smart optimized zero energy buildings: Energy, environment and economic assessments. *Sustainable Energy Technologies and Assessments, 48*, 101580.
42. Mithraratne, N. (2009). Roof-top wind turbines for microgeneration in urban houses in New Zealand. *Energy and Buildings, 41*(10), 1013-1018.
43. Kumar, N., & Prakash, O. (2023). Analysis of wind energy resources from high rise building for micro wind turbine: A review. *Wind Engineering, 47*(1), 190-219.
44. Peacock, A. D., Jenkins, D., Ahadzi, M., Berry, A., & Turan, S. (2008). Micro wind turbines in the UK domestic sector. *Energy and buildings, 40*(7), 1324-1333.
45. Bahaj, A. S., Myers, L., & James, P. A. B. (2007). Urban energy generation: Influence of micro-wind turbine output on electricity consumption in buildings. *Energy and buildings, 39*(2), 154-165.
46. Kazanci, O. B., Skrupskelis, M., Sevela, P., Pavlov, G. K., & Olesen, B. W. (2014). Sustainable heating, cooling and ventilation of a plus-energy house via photovoltaic/thermal panels. *Energy and Buildings, 83,* 122-129.
47. Bee, E., Prada, A., Baggio, P., & Psimopoulos, E. (2019, June). Air-source heat pump and photovoltaic systems for residential heating and cooling: Potential of self-consumption in different European climates. In *Building Simulation* (Vol. 12, No. 3, pp. 453-463). Beijing: Tsinghua University Press.
48. Martin-Escudero, K., Salazar-Herran, E., Campos-Celador, A., Diarce-Belloso, G., & Gomez-Arriaran, I. (2019). Solar energy system for heating and domestic hot water supply by means of a heat pump coupled to a photovoltaic ventilated façade. *Solar*

Energy, 183, 453-462.
49. Simko, T., Luther, M. B., Li, H. X., & Horan, P. (2021). Applying solar PV to heat pump and storage Technologies in Australian Houses. *Energies, 14*(17), 5480.
50. Du, W., Wang, J., Feng, Y., Duan, W., Wang, Z., Chen, Y., ... & Pan, B. (2023). Biomass as residential energy in China: Current status and future perspectives. *Renewable and Sustainable Energy Reviews, 186,* 113657.
51. Las-Heras-Casas, J., López-Ochoa, L. M., Paredes-Sánchez, J. P., & López-González, L. M. (2018). Implementation of biomass boilers for heating and domestic hot water in multi-family buildings in Spain: Energy, environmental, and economic assessment. *Journal of Cleaner Production, 176,* 590-603.
52. Palomba, V., Borri, E., Charalampidis, A., Frazzica, A., Cabeza, L. F., & Karellas, S. (2020). Implementation of a solar-biomass system for multi-family houses: Towards 100% renewable energy utilization. *Renewable energy, 166*, 190-209.
53. Allouhi, A., Rehman, S., & Krarti, M. (2021). Role of energy efficiency measures and hybrid PV/biomass power generation in designing 100% electric rural houses: a case study in Morocco. *Energy and Buildings, 236*, 110770.
54. Allouhi, A. (2022). Techno-economic and environmental accounting analyses of an innovative power-to-heat concept based on solar PV systems and a geothermal heat pump. *Renewable Energy, 191,* 649-661.
55. Antonijevic, D., & Komatina, M. (2011). Sustainable sub-geothermal heat pump heating in Serbia. *Renewable and Sustainable Energy Reviews, 15*(8), 3534-3538.
56. Ozgener, O. (2010). Use of solar assisted geothermal heat pump and small wind turbine systems for heating agricultural and residential buildings. *Energy, 35*(1), 262-268.
57. Tagliabue, L. C., Maistrello, M., & Del Pero, C. (2012). Solar heating and air-conditioning by GSHP coupled to PV system for a cost effective high energy performance building. *Energy Procedia, 30*, 683-692.
58. Kazanci, O. B., Skrupskelis, M., Sevela, P., Pavlov, G. K., & Olesen, B. W. (2014). Sustainable heating, cooling and ventilation of a plus-energy house via photovoltaic/thermal panels. *Energy and Buildings, 83*, 122-129.
59. Mitchell, J. W., & Braun, J. E. (2012). *Principles of heating, ventilation, and air conditioning in buildings.* John Wiley & Sons.
60. Romano, R., Siano, P., Acone, M., & Loia, V. (2017). Combined operation of electrical loads, air conditioning and photovoltaic-battery systems in smart houses. *Applied Sciences, 7*(5), 525.
61. Asim, N., Badiei, M., Mohammad, M., Razali, H., Rajabi, A., Chin Haw, L., & Jameelah Ghazali, M. (2022). Sustainability of heating, ventilation and air-conditioning (HVAC) systems in buildings—An overview. *International journal of environmental research and public health, 19*(2), 1016.
62. McQuiston, F. C., Parker, J. D., Spitler, J. D., & Taherian, H. (2023). *Heating, ventilating, and air conditioning: analysis and design*. John Wiley & Sons.
63. Kalaiselvam, S., & Parameshwaran, R. (2014). *Thermal energy storage technologies for sustainability: systems design, assessment and applications*. Elsevier.
64. Parameshwaran, R., Kalaiselvam, S., Harikrishnan, S., & Elayaperumal, A. (2012). Sustainable thermal energy storage technologies for buildings: A review. *Renewable and Sustainable Energy Reviews, 16*(5), 2394-2433.
65. Cruickshank, C. A., & Harrison, S. J. (2010). Heat loss characteristics for a typical solar domestic hot water storage. *Energy and buildings, 42*(10), 1703-1710.
66. Cabeza, L. F. (2021). Advances in thermal energy storage systems: Methods and applications. In *Advances in thermal energy storage systems* (pp. 37-54). Woodhead publishing.
67. Novo, A. V., Bayon, J. R., Castro-Fresno, D., & Rodriguez-Hernandez, J. (2010). Review of seasonal heat storage in large basins: Water tanks and gravel–water pits. *Applied Energy, 87*(2), 390-397.
68. Reuss, M., Beck, M., & Müller, J. P. (1997). Design of a seasonal thermal energy storage in the ground. *Solar energy, 59*(4-6), 247-257.
69. Zhu, N., Hu, P., Xu, L., Jiang, Z., & Lei, F. (2014). Recent research and applications of ground source heat pump integrated with thermal energy storage systems: A review. *Applied thermal engineering, 71*(1), 142-151.
70. Wang, H., Qi, C., Wang, E., & Zhao, J. (2009). A case study of underground thermal storage in a solar-ground coupled heat pump system for residential buildings. *Renewable energy, 34*(1), 307-314.
71. Pavlov, G. K., & Olesen, B. W. (2011). Seasonal ground solar thermal energy storage-review of systems and applications. In *ISES Solar World Congress 2011* (pp. P-1).
72. Pavlov, G. K., & Olesen, B. W. (2012). Thermal energy storage—A review of concepts and systems for heating and cooling applications in buildings: Part 1—Seasonal storage in the ground. *Hvac&R Research, 18*(3), 515-538.
73. Manual bat greenheiss gh-li 4.8 plus.indd .
74. Armenta-Déu, C. and Arenas, J. (2025) Improving Indoor Room Air Conditioning Using PID Control. Journal of Refrigeration, Air Conditioning, Heating and Ventilation, Volume 12, Issue 1, pages 1-21
75. Armenta-Déu, C. (2024). Application of artificial intelligence (AI) and home automation to energy saving in buildings. *International Journal of Sustainable Real Estate and Construction Economics, 3*(1), 1-26.
76. Armenta-Déu, C. (2022). Analysis of geological structure for the application of geotechnical engineering to optimize thermal

extraction in geothermal wells. *International Journal of Geological and Geotechnical Engineering, 8*(2), 26-35.
77. Svoboda, J. A., & Dorf, R. C. (2013). *Introduction to electric circuits*. John Wiley & Sons.
78. Bergman, T. L. (2011). *Fundamentals of heat and mass transfer*. John Wiley & Sons.
79. Armenta-Déu, C., Carriquiry, J.P., Guzmán, S. (2019) Capacity correction factor for Li-ion batteries: Influence of the discharge rate. Journal of Energy Storage, Volume 25, October 2019, 100839.
80. pyranometer-dts-v1a-DRAFT.cdr
81. Ficha Técnica Inversor Greenheiss Serie GH-IT 2M Y 2M-15
82. PCE-PA6000 Power Analyzer
83. Saunier Duva, 0020297943_00.pdfl
84. PicoLog TC-08 high-resolution thermocouple data logger
85. Ecoforest, ecoGEO + 1-9